J Solid State Electrochem (2014) 18:3327–3337
DOI 10.1007/s10008-014-2643-4

ORIGINAL PAPER

Electrochemical and nanogravimetric studies of iron phthalocyanine microparticles immobilized on gold in acidic and neutral media

Ákos Nemes · György Inzelt

Received: 27 June 2014 / Revised: 8 September 2014 / Accepted: 17 September 2014 / Published online: 13 November 2014

Abstract An electrochemical quartz crystal nanobalance has been used to study the redox behavior of iron phthalocyanine (FePc) microparticles attached to gold in contact with acidic and neutral aqueous solutions at different pH values in the absence and presence of oxygen, respectively. Five redox transformations have been detected: one has been assigned to the Fe^{2+}/Fe^{3+} redox process, while four of those have been assigned to the oxidation and reduction of the Pc ring; however, the reduction of Fe^{2+} and the reoxidation of Fe^{+} cannot be entirely excluded at potentials more negative than ca. −0.4 V vs. saturated calomel electrode (SCE). The redox processes are accompanied with significant mass changes which are related to the sorption and desorption of counterions and solvent molecules. An extensive solvent swelling occurs. The relatively slow motion of solvent molecules introduces a substantial scan rate dependence regarding the mass change during potential cycling. Due to the participation of H^{+} ions, the processes related to the oxidation and reduction of the Pc ring show pH dependence. Simultaneous with the charge transfer processes, solid-solid phase transitions can be assumed, especially in the case of the redox transformations occurring at most cathodic potentials. The mass change that can be detected in the presence of oxygen indicates a bonding of oxygen to FePc. During a cathodic voltammetric scan, the reduction of oxygen (ORR) starts when the central iron (III) ion of FePc is converted to Fe(II) during reduction. It follows that the electrocatalytic efficiency of FePc, which is comparable with that of Pt in acid and neutral solutions, cannot be expected at even lower overpotentials because the redox transformation of the central Fe ion of FePc determines the rate of the ORR.

Keywords Iron phthalocyanine · Microparticles · Electrochemical quartz crystal nanobalance (EQCN) · Redox transformations · Solid-solid phase transition · Oxygen reduction

Introduction

The first phthalocyanine (iron phthalocyanine) was discovered by chance in 1928 during the industrial production of phthalimide, and it was first studied by Linstead in detail. Linstead published a series of papers devoted to the preparation and characterization of several phthalocyanines, and he also proposed the structure of this class of compounds [1, 2]. Investigations of the electrochemical behavior of phthalocyanines have been in the foreground of research during the last 30 years ([3–54] and citations therein) especially as a catalyst of the oxygen reduction reaction (ORR) since it is of utmost importance to find a suitable and cheap catalyst which could replace the expensive platinum [6, 11, 12, 15, 18, 33, 43, 45, 47, 49, 51, 52, 54]. A wide range of other applications besides catalysis such as in electrochromic display devices [13, 14], in electrochemical power sources including solar cells [28, 43, 47, 49], and in sensors [21, 31, 32, 41] has also been put forward. However, the elucidation of the electrochemical processes occurring during the redox transformations of phthalocyanines is an interesting and challenging task in itself. In the literature, very diverse cyclic voltammograms can be found even for the same metal phthalocyanine. The main reason is that the voltammetric and other (e.g., spectroscopic) responses of phthalocyanine ring (Pc) strongly depend on metal ions in the center of the ring, the substituents on the periphery of the

This paper is dedicated to Professor Stephen Fletcher on the occasion of his 65th birthday.

Á. Nemes · G. Inzelt (✉)
Department of Physical Chemistry, Institute of Chemistry, Eötvös Loránd University, Pázmány Péter sétány 1/A, Budapest 1117, Hungary
e-mail: inzeltgy@chem.elte.hu

macrocyclic ring, the solvent and the electrolyte used (especially when complex forming agents are present), the presence of oxygen, temperature, and even the morphology of the surface layer (adsorbed or deposited by different methods). A further difficulty of the comparison of the results is that in the majority of the cases, substituted phthalocyanines [5, 11, 22, 38, 44, 45, 48, 50] were used to make the compound soluble. Several processes including irreversible ones can take place such as the formation of peroxy and oxo-bridged species in contact with oxygen in solution or even in solid form, or nucleation growth-like phase transition in the solid layer during redox processes. The variety of the shape of the voltammograms is due to thermodynamic reasons and also to the kinetic effects.

According to theoretical considerations, if the metal *d* orbitals are positioned between HOMO and LUMO gap of the phthalocyanine (Pc^{2-}) ligand, e.g., it is the case for Co and Fe, the redox transformation of the central metal ion can be observed especially if suitable coordinating species are present in the solution. For other metal phthalocyanines such as Cu, Ni, Zn, Pt, and Pd, the metal ions do not participate in the redox processes, and only the Pc ring will be oxidized or reduced [15, 16, 31, 32]. A wide arsenal of nonelectrochemical methods has been used to characterize the different phthalocyanines; however, the electrochemical quartz crystal nanobalance (EQCN) has not been exploited; yet, only limited studies have been carried out on platinum phthalocyanine [29], palladium phthalocyanine [36, 53], and α-FePc [52]. Because the results of EQCN experiments can provide different, valuable information of the electrochemical transformations of solid particles immobilized on metal surfaces [55–62], in the present study, we focus our attention on the EQCN study of iron phthalocyanine (FePc) microparticles attached to gold and investigated under different conditions.

Experimental

FePc (Alfa Aesar 96 %) was used without further purification. Analytical grade chemicals such as H_2SO_4 (Merck), HCl (Sigma-Aldrich), Na_2SO_4 (Merck), and $FeSO_4 \cdot 7H_2O$ (Merck) were used as received. Doubly distilled water was used (Millipore water). All solutions, except the oxygen reduction studies, were purged with oxygen-free argon (purity 5.0, Linde Gas Hungary Co. Cltd.), and an inert gas blanket was maintained throughout the experiments. A sodium chloride saturated calomel electrode (SCE) was used as the reference electrode which was carefully separated from the main compartment by using a double frit. A gold wire served as the counter electrode. The cycling of the potential as a pretreatment of the electrode was carried out before each experiment in the supporting electrolyte, until a voltammogram characteristic to the clean gold electrode was obtained. Fe-phthalocyanine microparticles were immobilized on the gold surface from a sonicated Fe-phthalocyanine-isopropanol sol via dropping an adequate amount of the suspension and drying it. The sonification was made by a Realsonic 57, Korea. (Mechanical abrasion method was also used to deposit FePc layer on EQCN electrode. Albeit similar voltammetric and EQCN responses were obtained also for these layers, it was more difficult to control the amount attached to the electrode surface; therefore, these results are not reported herein.)

Five megahertz AT-cut crystals of 1 inch diameter coated with gold or platinum (Stanford Research Systems, SRS, USA) were used in the EQCN measurements. The electrochemically and the piezoelectrically active areas were equal to 1.37 and 0.4 cm^2, respectively.

The Sauerbrey equation [56] was used to relate the surface mass change (Δm) to the frequency shift (Δf):

$$\Delta f = -C_f \Delta m / A \tag{1}$$

The integral sensitivity of the crystals (C_f) was found to be 56.6×10^6 Hz g^{-1} cm^2, i.e., 1 Hz corresponds to 17.7 ng cm^{-2}. The integral sensitivity was calculated by using the frequency change and the charge measured during silver deposition/dissolution as well as for the electroreduction of gold oxide in order to determine the real surface area of the electrode. The apparent molar mass of the deposited or the exchanged species (M) was calculated from the slope of the Δf vs. Q curve using the following formula:

$$M = (nFA/C_f)\mathrm{d}\Delta f/\mathrm{d}Q \tag{2}$$

where n is the number of electrons involved in the electrochemical reaction, F is the Faraday constant, Δf is the frequency change, Q is the charge consumed, and A is the electrode surface area. Although the requirements (uniform and homogeneous surface layer) for the application of Sauerbrey equation are not perfectly met, on the basis of measured frequency values, a rough estimation can be done. The relative values of Δf obtained for the incorporation of different ions and solvent molecules, however, should be approximately correct. The crystals were mounted in the holder made from Kynar and connected to a SRS QCM 200 unit. Either an Elektroflex 453 potentiostat or a Biologic VSP potentiostat and a Universal Frequency Counter PM6685 (Fluke) connected to an IBM personal computer were used for the control of the measurements and for the acquisition of the data.

Simultaneous with the frequency, the motional series resistance (loss), which changes with the change of viscosity/elasticity of the material (film or liquid) in contact with the crystal surface, was also monitored. Because it remained constant, the behavior of the surface layer consisting of microparticles remained elastic during the electrochemical transformations, i.e., no viscoelastic effect appeared. The deposited

layers were also investigated by focused ion beam scanning electron microscope (FIB-SEM) type FEI Quanta 3D, the Netherlands.

Results and discussion

The distribution of Fe-phthalocyanine microparticles on the gold surface

Figure 1 shows that Fe-phthalocyanine microparticles, deposited from a sonicated Fe-phthalocyanine-isopropanol sol, cover the surface of the gold. The diameter of the individual particles is between 20 and 80 nm, and their length is between 100 and 250 nm. After cyclic voltammetric experiments, more agglomerates can be seen (Fig. 1b).

Solvent sorption

The sorption of water in the layer either in bounded form or as a consequence of physical swelling by electrolyte solution is indicated by the higher decrease of the frequency in comparison with the frequency decrease after immersion of uncoated QCN gold electrodes in the same solution. For a gold electrode, 900–1,000 Hz decrease was measured, which is the expected value due to the solution effect which is proportional to the viscosity and the density of the contacting media. For Au|FePc electrodes—depending on the layer thickness—from −1,500 to −2,100 Hz was measured. It is in accordance with the results of the X-ray (EXAFS and XANES) experiments which have been explained by the formation of an octahedral $(H_2O)_2Fe^{2+}Pc^{2-}$ as a consequence of the interactions between FePc and water molecules in acidic solutions [52].

Au|FePc electrodes in deaerated acidic solutions

The properties of the Fe^{2+}/Fe^{3+} redox waves

Our first intention was to test the redox response of the central ion. Figure 2 shows cyclic voltammograms and the simultaneously obtained EQCN curves for FePc microparticles deposited on gold in contact with deaerated sulfate containing pH 2 solution in the potential region of −0.1 and 0.6 V. The anodic peak at 0.31 V and the cathodic peak at 0.278 V (waves III_a and III_c) belong to the Fe^{2+}/Fe^{3+} redox transformations. In the whole potential region investigated, i.e., between −0.5 and 1.3 V, five main redox processes were observed; therefore, the peaks were numbered from I to V, where I is the peak detected at most positive potentials.

The position of these peaks somewhat depends on the scan direction as seen in Fig. 3. It can be related to the kinetics of the formation of different species and also to an ohmic drop effect, since the conductivity of the layer substantially depends on its oxidation state (Nemes et al., 2014, unpublished results).

Second waves—whose peak potentials also depend on the scan direction—are well seen when the positive potential limit was extended until 0.8 V. Besides the anodic wave, a cathodic wave also appears in this potential region whose intensity depends on the delay time at 0.8 V. The further oxidation (wave II_a) starting at ca. 0.5 V in the pH range from 0 to 2 can be related to the oxidation of the dimeric species [7, 42, 52] forming during the oxidation.

For a simple Fe^{2+}/Fe^{3+} redox transformation, no pH dependence is expected. Comparing the curves in Figs. 2 and 3, a shift of ca. −20 mV/pH is obtained for the peak potentials when the cycle was started from −0.1 V.

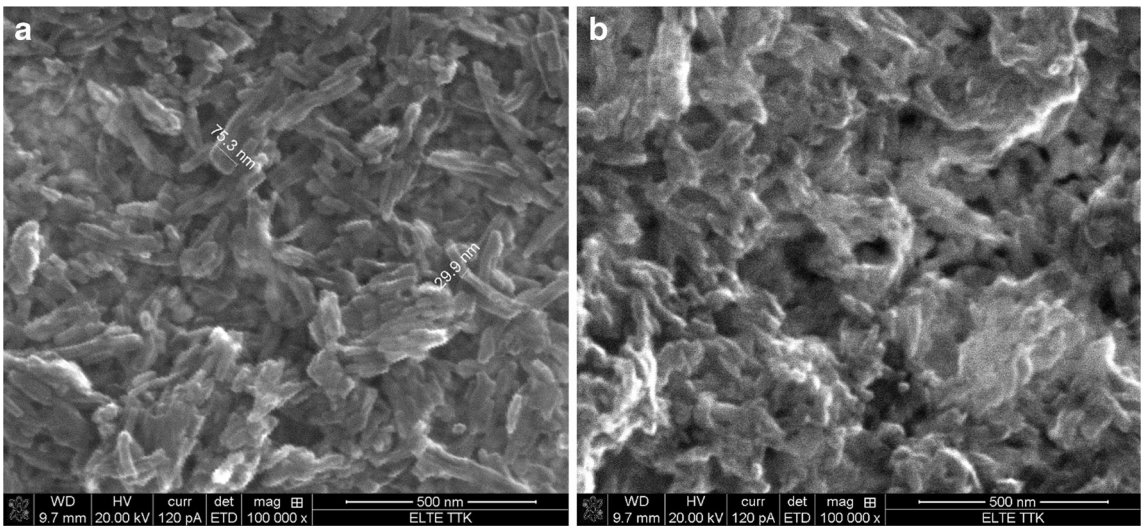

Fig. 1 SEM pictures of the EQCN gold electrode covered with Fe-phthalocyanine microparticles: **a** freshly prepared layer, **b** after cyclic voltammetric investigations

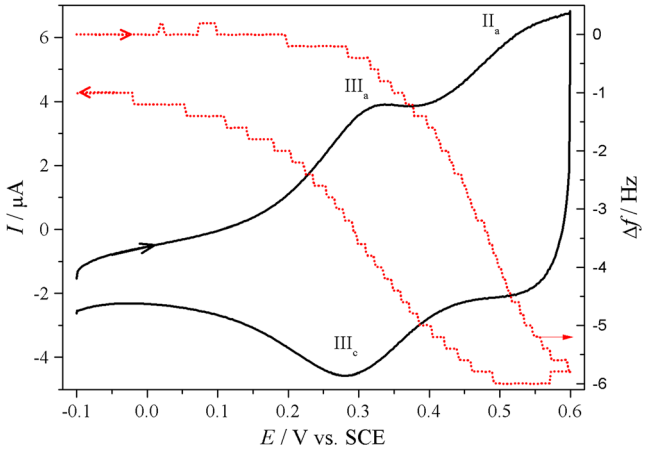

Fig. 2 Cyclic voltammetric and the simultaneously obtained EQCN frequency responses for an Au|FePc electrode in contact with 0.5 mol dm^{-3} deaerated pH 2 (H_2SO_4/Na_2SO_4) buffer. Positive potential limit is 0.6 V. Scan rate=20 mV s^{-1}

The pH dependence, however, can be proven when studying a wider pH range while keeping the potential interval—at least approximately—in the same potential range on the relative hydrogen electrode scale. It is of importance because further reduction or oxidation processes of the Pc ring influence the voltammetric responses (see below).

From the EQCN results, M=46±15 g mol^{-1} and M=116±15 g mol^{-1} in the first and second phases of oxidation, respectively, were calculated. It can be concluded that anions enter the layer and water sorption also occurs. However, it should be mentioned that this molar mass values can be calculated for the layers after several cycles. Depending on the layer thickness, for an unused layer, higher frequency decrease can be observed, and consequently, higher M values come about since the charge does not increase proportionally during subsequent cycles.

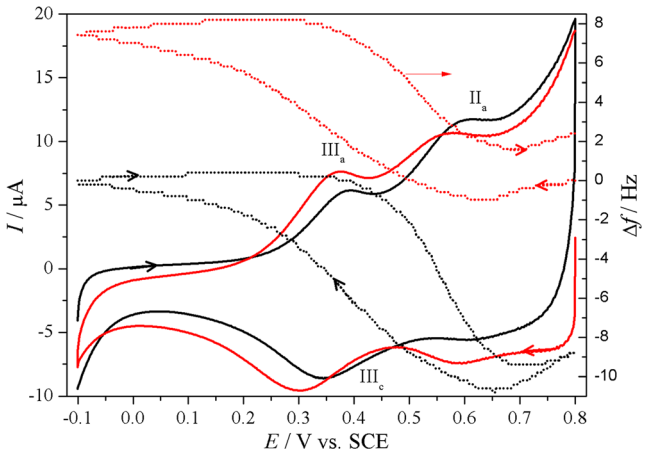

Fig. 3 Cyclic voltammetric and the simultaneously obtained EQCN frequency responses for an Au|FePc electrode at different scan directions. Positive potential limit is 0.8 V. Electrolyte is 0.5 mol dm^{-3} sulfuric acid. Scan rate=20 mV s^{-1}

It follows that a substantial amount of water molecules enters the surface layer during the first cycles.

The anodic and cathodic peaks belonging to the Fe^{2+}/Fe^{3+} redox transformations appear at 0.41 and at 0.36 V, respectively, when 5 mol dm^{-3} sulfuric acid (Hammett acidity function, H_o=−2.28) was used as an electrolyte (Fig. 4), i.e., a slight positive shift of the peak potentials can be observed. It is also true for wave II$_a$. However, the waves belonging to the redox transformations of the Pc ring (wave IV) are seemingly more sensitive to the pH change; E_{pa} (IV) appears at +0.04 V, while it is around −0.125 V in 0.5 M sulfuric acid. The calculated molar mass values of the exchanged species are less that those in more dilute sulfuric acid, indicating that a decrease of the water activity causes a decrease of solvent sorption.

In order to get information on the participation of the anions, the same layer was studied in both H_2SO_4 and HCl solutions (Fig. 5). The molar mass values calculated in the case of sulfuric and hydrochloride acids, respectively, were proportional to the molar masses of anions at waves III$_a$ and II$_a$ attesting the incorporation of the charge-compensating counterions during oxidation. However, the ratio of molar masses decreases with decreasing scan rate, indicating that the slower moving water molecules also enter the layer and the water sorption is higher in the case of chloride ions than that of sulfate ions (Fig. 5a, b).

Effect of the potential limits: the redox transformations of the phthalocyanine ring

Further increase of the positive potential limit eventually leads to the dissolution of the FePc layer due to the oxidation of the Pc ring (Pc^{2-}/Pc^{-} couple). The results obtained for a freshly deposited FePc layer when the positive potential limit was set to 1.3 V are shown in Fig. 6.

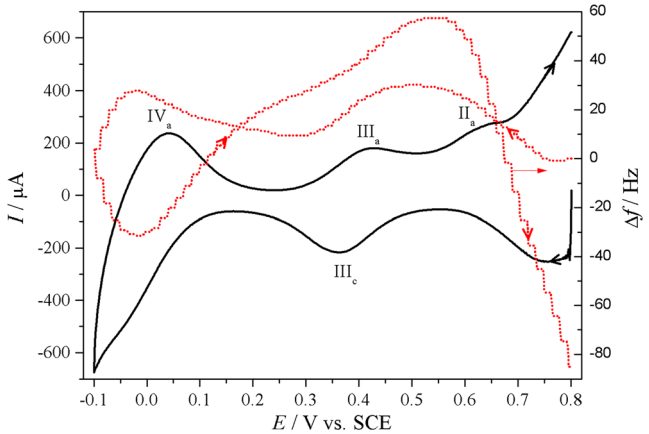

Fig. 4 Cyclic voltammetric and the simultaneously obtained EQCN frequency responses for Au|FePc electrode in contact with 5 mol dm^{-3} sulfuric acid. Scan rate=50 mV s^{-1}

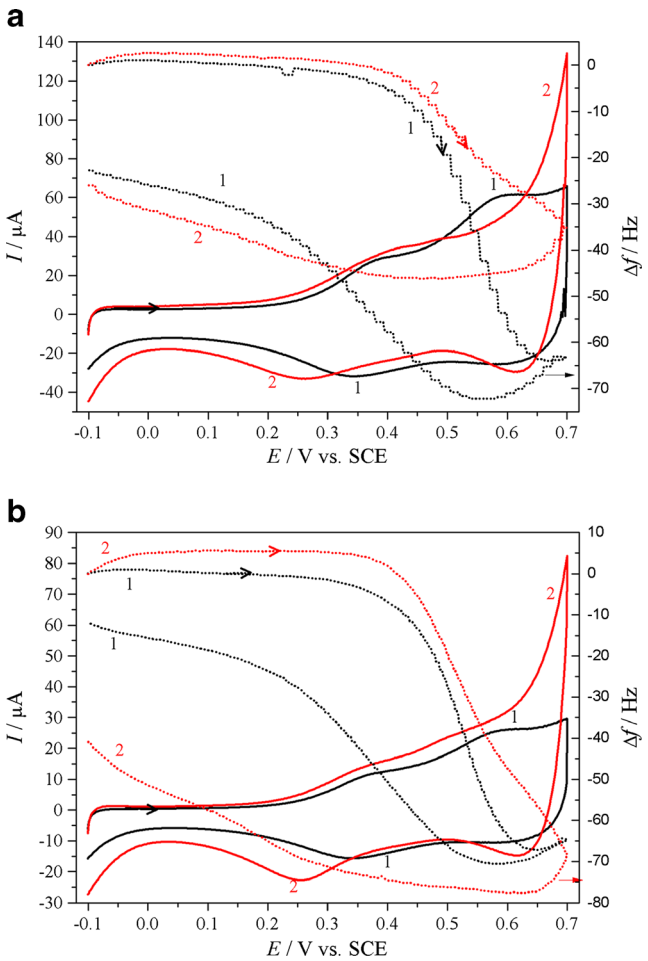

Fig. 5 Cyclic voltammetric and the simultaneously obtained EQCN frequency responses for Au|FePc electrode in contact with 0.5 mol dm^{-3} sulfuric acid (*1*) and hydrochloric acid (*2*), respectively. Scan rates=50 mV s^{-1} (**a**) and 20 mV s^{-1} (**b**)

Until ca. 0.95 V, i.e., ca. at the peak potential of the high, irreversible oxidation wave, only mass increase can be observed; however, it is followed by a substantial mass loss (Fig. 6). Albeit certain mass increase occurs below ca. 0 V, eventually, the surface layer will be dissolved. (Most likely a substantial part of the mass increase during the reverse scan is due to the sorption of water, while FePc particles detached from the surface.) Therefore, we restricted our studies to the potentials below 0.8 V.

With the extension of the negative potential limit, a new pair of waves (waves IV_a and IV_c) appears at ca. −0.2 V accompanied with mass decrease and mass increase during the anodic and cathodic scans, respectively (Fig. 7). These waves are related to the redox reaction of the Pc ring belonging to Pc^{2-}/Pc^{3-} couple [7, 42, 52]. In the simplest case counterions, H^+ or Na^+ (in solutions containing Na_2SO_4) enters and leaves the layer during reduction and oxidation, respectively.

According to the EQCN frequency change, however, the observed molar mass values, i.e., M=42±15 g mol^{-1} in sulfuric acid solutions or M=80±15 g mol^{-1} in Na_2SO_4, could only be explained if water sorption is also assumed. In acid solutions, it can be expected that reduced phthalocyanine is at least partially protonated [53], and in this case, besides the transport of hydrogen ions, anions also participate in the charge-compensating process. Furthermore, the pH dependence also indicates the participation of protons in the electrode reaction.

At more negative potentials, other redox transformations occur as seen in Fig. 8. This pair of waves dominates the cyclic voltammograms, and very high mass decrease and mass increase can be observed both in anodic and cathodic directions, respectively. This pair of waves (V_a and V_c) belongs to the further reduction of the Pc ring; however, the reduction of Fe^{2+} and the reoxidation of Fe^+ cannot be entirely excluded [32, 52]. The mass changes take place in two steps. At potentials more negative than ca. −0.4 V, further reduction occurs, which causes an initial mass increase after keeping the potential at −0.5 V, and then starting the cycle from this potential. In

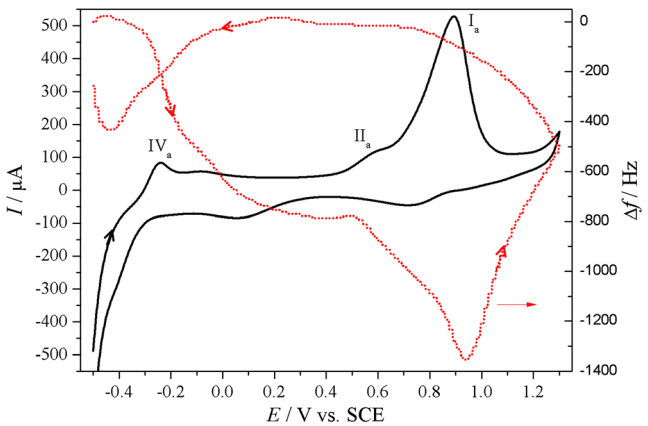

Fig. 6 Cyclic voltammetric and the simultaneously obtained EQCN frequency responses for an Au|FePc electrode in contact with 0.5 mol dm^{-3} sulfuric acid. Positive potential limit is 1.3 V. Scan rate= 50 mV s^{-1}

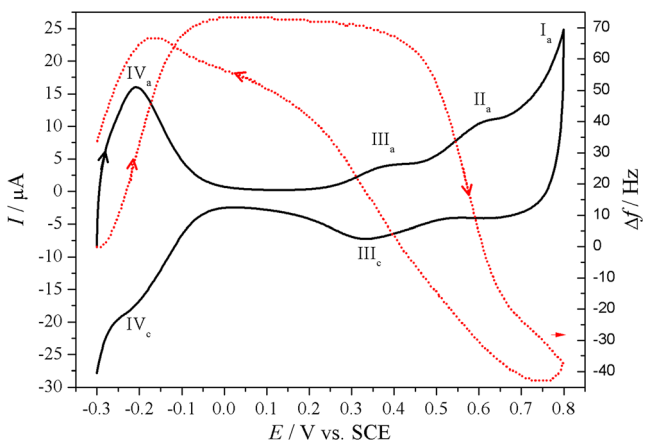

Fig. 7 Cyclic voltammetric and the simultaneously obtained EQCN frequency responses for an Au|FePc electrode. Cathodic potential limit is −0.3 V. Electrolyte is 0.5 mol dm^{-3} sulfuric acid. Scan rate=10 mV s^{-1}

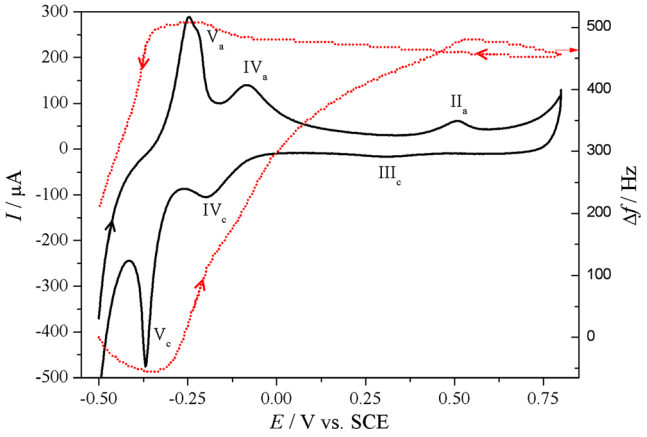

Fig. 8 Cyclic voltammetric and the simultaneously obtained EQCN frequency responses for an Au|FePc electrode. Cathodic potential limit is −0.5 V. Electrolyte is 0.5 mol dm^{-3} sulfuric acid. Scan rate=10 mV s^{-1}

this case, the frequency increase will be drawn out during the positive-going scan.

The frequency change is getting higher and higher as the cycle was started at more and more negative potentials. It is also remarkable that wave II_a at ca. 0.6 V is also affected by the starting potential, which indicates that at low potentials, drastic changes of the structure of FePc microparticles occur, which manifests itself also in the hysteresis of EQCN response.

The further reduction and reoxidation at waves V_c and V_a cannot be described by the a simple equation considering further sorption of cations because this wave is also pH dependent. In order to get information on the kinetics of the processes, scan rate dependence has also been studied. Figure 9 shows the effect of scan rate on the cyclic EQCN response. According to the scan rate dependence of the peak currents, the waves observed are surface ones. The scan rate dependence of the EQCN frequency response reveals that the redox transformations are accompanied with slow sorption-desorption processes. It is usually explained by the motion of the neutral solvent molecules, while the potential-driven migration of ions is fast. It should be mentioned that the uptake of a large amount of solvent can cause a substantial change of the structure of the microparticles. Phase transitions are also accompanied with extensive swelling-deswelling of the surface layer, while the stress arising in the surface layer can affect the EQCN response substantially [58–62]. The latter effect certainly prevents the derivation of reliable values for the mass change. These effects which cause the large hysteresis are even more obvious when a larger potential window is used.

Au|FePc electrodes in deaerated Na_2SO_4 solutions

In Fig. 10, cyclic voltammetric and the simultaneously obtained EQCN frequency responses for an Au|FePc electrode in contact with 0.5 mol dm^{-3} Na_2SO_4 are presented. It is evident that pH dependence of waves III_a and III_c that belong to the Fe^{2+}/Fe^{3+} redox transformations is negligible since the peak potentials are practically the same that was observed in the pH interval from 0 to 2 (Figs. 2 and 3). From the peak potentials of waves IV_a and IV_c, ca. −30 mV/pH in weakly acidic and neutral solutions and ca. −55 mV/pH for pH values below 0 can be calculated by using the data obtained for H_o=−2.28, pH 0, pH 0.3, pH 1, pH 2, and pH 7. It means that besides Na^+ ions, H^+ ions also participate in the redox reactions. However, the shift of the peaks depends on the pH which indicates that the protonation of the Pc ring depends on the acidity of the contacting solution, and a pK_a value for the reduced Pc ring close to 0 can be estimated. It follows that the reduced Pc ring only partially protonated at higher pH values.

Scheme of the redox transformations

In order to give a reasonable scheme of the redox transformations, we have to take into account both the mass changes and the pH dependence of the peaks observed. Furthermore, it is also instructive that immersing the Au|FePc EQCN electrode in the acidic electrolyte, an excess frequency change can be observed which may relate to the sorption of water. Water molecules as ligands can form an octahedral $(H_2O)_2Fe^{2+}Pc^{2-}$ complex with FePc [42]. In acid solutions, partial protonation of the nitrogen atoms of the Pc ring can also occur, and to maintain the electroneutrality, anions enter the layer.

Therefore, before any potential cycling, we have to consider at least four forms of FePc, i.e., $Fe^{2+}Pc^{2-}$, $(H_2O)_2Fe^{2+}Pc^{2-}$, $Fe^{2+}Pc^{2-}H^+HSO_4^-$, and $(H_2O)_2Fe^{2+}Pc^{2-}H^+HSO_4^-$ in the solid phase(s). In the surface layer, there may be a mixture of these species.

Wave III and wave II (Fe^{2+}/Fe^{3+} transitions)

At wave III, the following data have to be considered: –20± 5 mV/pH, M=46±15 g mol^{-1} (at the beginning), and 116± 10 g mol^{-1} (after the peak potential). As it has been assumed in several papers [10, 13, 14, 20, 29], we can consider the incorporation of the charge-compensating counterions at least in the second half of the wave since minor pH dependence was observed:

$$Fe^{2+}Pc^{2-}(s) + HSO_4^-(aq) \rightleftarrows Fe^{3+}Pc^{2-}HSO_4^-(s) + e^- \quad (3)$$

however, at the beginning

$$Fe^{2+}Pc^{2-}(s) + H_2O(aq) \rightleftarrows Fe^{3+}Pc^{2-}OH^-(s) + H^+(aq) + e^- \quad (4)$$

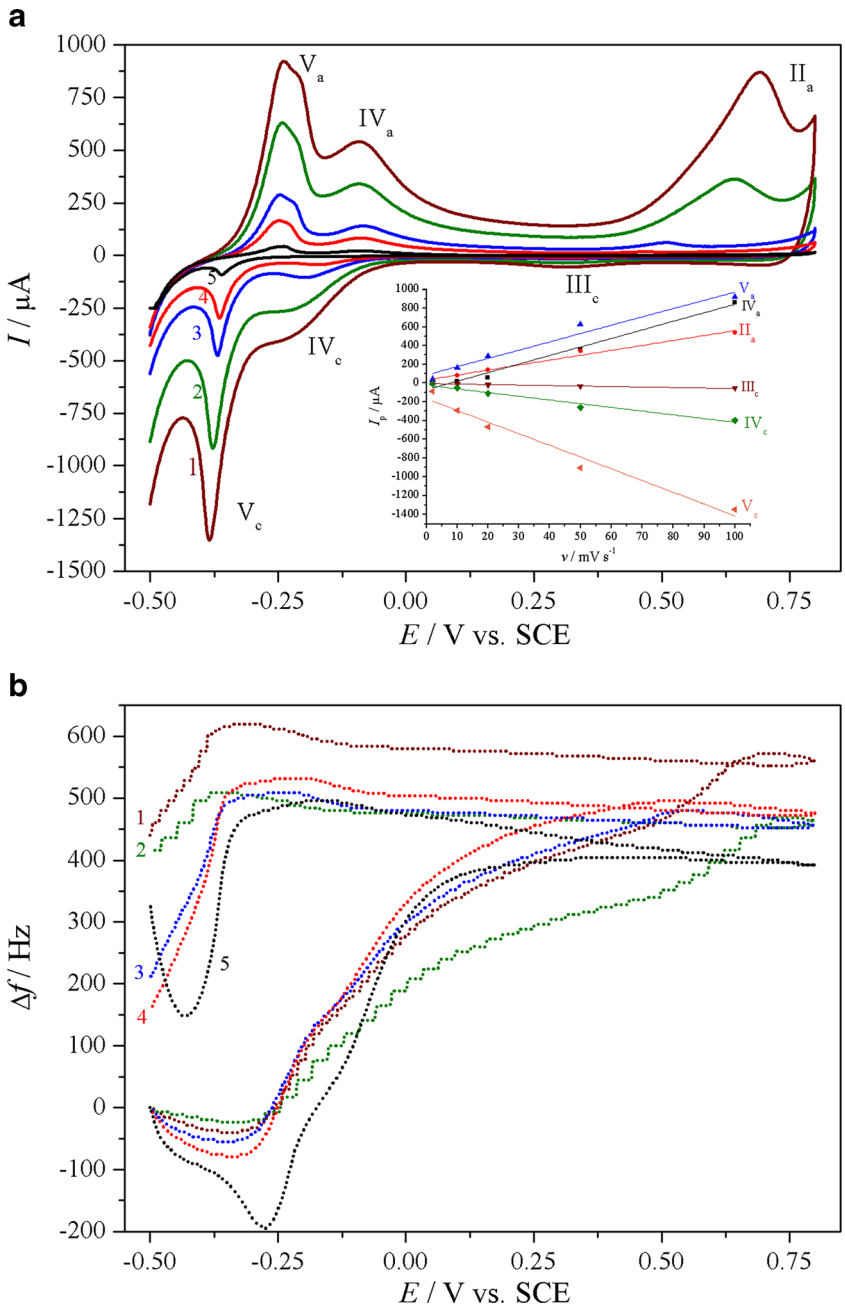

Fig. 9 Scan rate dependence of the cyclic voltammetric (**a**) and the simultaneously obtained EQCN frequency responses (**b**) for an Au|FePc electrode. Cathodic potential limit is −0.5 V. Electrolyte is 0.5 mol dm^{-3} sulfuric acid. Scan rates are as follows: 100 (*1*), 50 (*2*), 20 (*3*), 10 (*4*), and 2 mV s^{-1} (*5*). *Insert*: I_p vs. *v* function

(proposed in [52]) cannot be entirely neglected. Considering an aqua complex as the starting compound, similar dependences can be obtained:

$$(H_2O)_2Fe^{2+}Pc^{2-}(s) + HSO_4^-(aq) \rightleftarrows (H_2O)_2Fe^{3+}Pc^{2-}HSO_4^-(s) + e^- \quad (5)$$

However, in this way, the pH dependence cannot be explained either. If we assume a dimerization reaction:

$$2Fe^{2+}Pc^{2-}(s) + H_2O(aq) + HSO_4^-(aq) \rightleftarrows Fe^{2+}Pc^{2-}\text{–O–}Fe^{3+}Pc^{2-}HSO_4^-(s) + 2H^+(aq) + 3e^- \quad (6)$$

both the pH dependence and the mass change are better explained. Furthermore, wave II (oxidation of a dimeric species [52]), where –7±5 mV/pH, M=123±10 g mol^{-1}, can also be easily interpreted by the following equation:

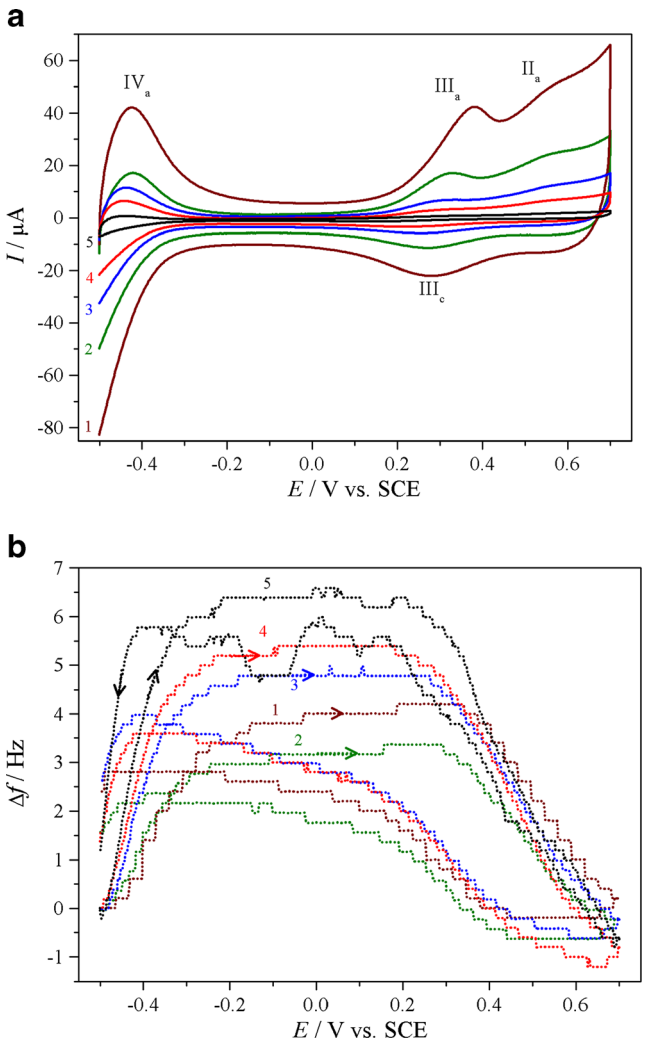

Fig. 10 Scan rate dependence of the cyclic voltammetric (**a**) and the simultaneously obtained EQCN frequency responses (**b**) for an Au|FePc electrode. Electrolyte is 0.5 mol dm^{-3} Na_2SO_4. Scan rates are as follows: 100 (*1*), 50 (*2*), 20 (*3*), 10 (*4*), and 2 mV s^{-1} (*5*)

$$Fe^{2+}Pc^{2-}\text{–}O\text{–}Fe^{3+}Pc^{2-}HSO_4^-(s) + HSO_4^-(aq) \rightleftarrows Fe^{3+}Pc^{2-}\text{–}O\text{–}Fe^{3+}Pc^{2-}(HSO_4^-)_2(s) + e^- \quad (7)$$

Wave I (Pc^{2-}/Pc^- couple)

The further oxidation, where M=144±20 g mol^{-1} was found, can be described as follows:

$$Fe^{3+}Pc^{2-}\text{–}O\text{–}Fe^{3+}Pc^{2-}(HSO_4^-)_2(s) + 2HSO_4^-(aq) \rightleftarrows Fe^{3+}Pc^-\text{–}O\text{–}Fe^{3+}Pc^-(HSO_4^-)_4(s) + 2e^- \quad (8)$$

Wave IV (Pc^{2-}/Pc^{3-}) and wave V (Pc^{3-}/Pc^{4-}) or (Fe^+/Fe^{2+})

For wave IV, the nature of the redox transformations could be derived from the following data: −55±10 mV/pH (in strongly acidic media) and −30±10 mV/pH (in weakly acidic and neutral solutions) and M=42±15 g mol^{-1} (H_2SO_4) and 80±15 g mol^{-1} (Na_2SO_4, after the peak potential). From the pH dependence, it follows that the protonation plays a role, and the pK_a value is around 0. For wave V, considering data obtained for pH 0.3 and pH 7, −95±10 mV/pH can be calculated and M=65±15 g mol^{-1} (H_2SO_4) and 82±15 g mol^{-1} (Na_2SO_4).

While the mass change could be explained by the incorporation of hydrated cations

$$Fe^{2+}Pc^{2-}(s) + e^- + C^+(aq) \rightleftarrows Fe^{2+}Pc^{3-}C^+(s) \quad (9)$$

where C^+=H^+ or Na^+ (in solutions containing Na_2SO_4) in acidic media. However, Eq. (9) does not describe the pH dependence.

Therefore, we have to assume the participation of the hydroxonium ions (protons) in the reaction

$$Fe^{2+}Pc^{2-}(s) + e^- + C^+(aq) + H^+(aq) + HSO_4^-(aq) \rightleftarrows Fe^{2+}Pc^{3-}C^+\ H^+HSO_4^-(s) \quad (10)$$

or in acid

$$Fe^{2+}Pc^{2-}(s) + e^- + 2H^+(aq) + HSO_4^-(aq) \rightleftarrows Fe^{2+}Pc^{3-}H^+{}_2HSO_4^-(s) \quad (11)$$

The reaction of an aqua complex can also be considered:

$$(H_2O)_2Fe^{2+}Pc^{2-}(s) + 2\ H^+(aq) + HSO_4^-(aq) + e^- \rightleftarrows (H_2O)Fe^{2+}Pc^{3-}H^+{}_2HSO_4^-(s) + H_2O(aq) \quad (12)$$

which gives a better description of the molar mass values because of the counterflux of ions and solvent molecules.

Wave V can be related to the formation of Pc^{4-} species. However, a rather minor mass change can be observed (a slight increase of frequency can be detected) during reduction until the peak potential of V_c peak, and a mass increase starts only after the wave. Similarly, during the oxidation, the frequency increase starts when the potential passes the peak V_a.

Consequently, no incorporation of heavy ions can be assumed in the first phase of this redox process, i.e., the following equation may be approximately valid:

$$(H_2O)Fe^{2+}Pc^{3-}H^{+}{}_2HSO_4{}^{-}(s) + e^{-} + H^{+}(aq) \rightleftarrows (H_2O)Fe^{2+}Pc^{4-}H^{+}{}_3HSO_4{}^{-}(s) \quad (13)$$

This reaction may be followed by the incorporation of cations (protons) and anions, i.e., a protonation equilibrium prevails:

$$(H_2O)Fe^{2+}Pc^{4-}H^{+}{}_3HSO_4{}^{-}(s) + H^{+}(aq) + HSO_4{}^{-}(aq) \rightleftarrows (H_2O)Fe^{2+}Pc^{4-}H^{+}{}_4(HSO_4{}^{-})_2(s) \quad (14)$$

However, in the potential range of peak IV and especially that of peak V, phase transition also occurs which manifests itself in the increase of the difference of the respective anodic and cathodic peak potentials, since this process needs extra energy and usually accompanied by sorption-desorption of solvent molecules [55, 58–62].

We may also consider the reduction of the central ion and a catalytic hydrogen evolution as it has been suggested for CoPc [38]:

$$(H_2O)Fe^{2+}Pc^{3-}H^{+}{}_2HSO_4{}^{-}(s) + e^{-} + H^{+}(aq) \rightleftarrows (H_2O)Fe^{+}Pc^{3-}H^{+}{}_3HSO_4{}^{-}(s) \quad (15)$$

$$(H_2O)Fe^{+}Pc^{3-}H^{+}{}_3HSO_4{}^{-}(s) + H^{+}(aq) \rightleftarrows (H_2O)Fe^{2+}Pc^{3-}H^{+}{}_2HSO_4{}^{-}(s) + H_2(g) \quad (16)$$

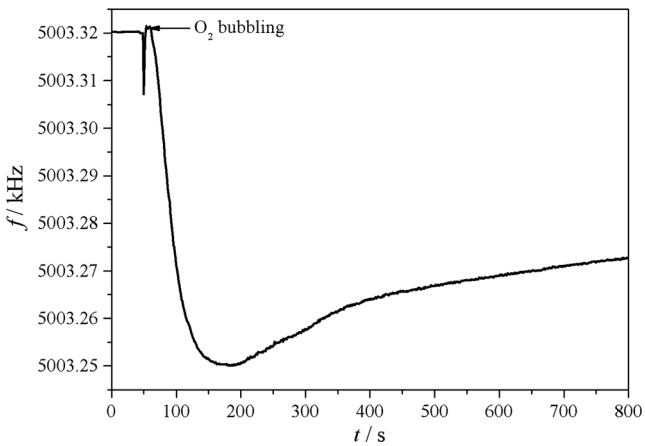

Fig. 11 The change of the EQCN frequency response of an Au|FePc electrode as a function of time during oxygen bubbling. Electrolyte is 0.5 mol dm^{-3} H_2SO_4

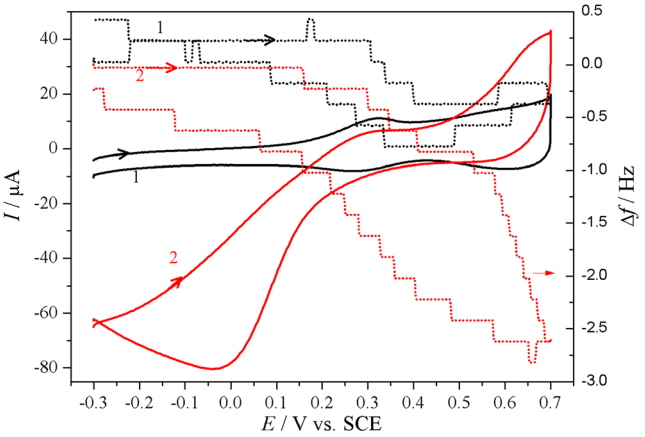

Fig. 12 Cyclic voltammetric and the simultaneously obtained EQCN frequency responses for a gold (*1*) and an Au|FePc (*2*) electrode in the presence of oxygen. Electrolyte is 0.5 mol dm^{-3} Na_2SO_4. Scan rate= 50 mV s^{-1}

Based on the EQCN data, a reduction to Fe^0 is not considered; however, it may take place at potentials below −0.5 V.

Link between oxygen reduction reaction (ORR) and redox transformation of the central (Fe^{2+}/Fe^{3+}) ion

In order to test the effect of oxygen and the catalytic ability of our FePc sample concerning ORR, measurements have been carried out in the presence of oxygen. In the detailed investigation shown above, oxygen was carefully excluded from the solutions used. EQCN results supply evidence that in the presence of oxygen, a mass increase can be observed (Fig. 11), which supports the assumption that FePc species forms adducts with O_2 [52, 54].

During a cathodic voltammetric scan, the reduction of oxygen (ORR) starts when the central iron (III) ion of FePc is converted to Fe(II) during reduction (Fig. 12). In the potential region of the oxygen reduction reaction, the EQCN frequency change does not differ from that observed in the absence of oxygen. Taking into account the beginning of the electroreduction of the oxygen during the cathodic scan, it can be concluded that Fe-phthalocyanine is almost as good catalyst as platinum in acid and neutral media since the decrease of overpotential is nearly the same. A detailed EQCN investigation is in progress to gain a deeper insight into the ORR catalyzed by FePc in acidic and basic media.

Conclusions

A deeper understanding of the electrochemical/electrocatalytic behavior of iron phthalocyanine is of utmost importance regarding its use as a cheap catalyst in oxygen reduction reaction

and for other practical purposes. The study of the potential-dependent ionic and solvent exchange processes by EQCN revealed the rather complex mechanism of the redox transformations of FePc microparticles attached to a gold surface, and the knowledge derived can be utilized in order to select the best conditions regarding the catalytic efficiency and the stability of the catalyst.

The shape of the cyclic voltammograms, i.e., the number of oxidation and reduction peaks and their relative ratios, depends on several factors such as the potential limits, presence and absence of oxygen, the nature and the concentration of the electrolyte, as well as the layer thickness. In aqueous acidic and neutral media, five redox processes of FePc can be distinguished. One of them belongs to the Fe^{2+}/Fe^{3+} couple, while four of them can be assigned to the redox transformations of the Pc ring; however, the reduction of Fe^{2+} and the reoxidation of Fe^{+} cannot be entirely excluded at potentials more negative than ca. −0.4 V. Fe^{2+}/Fe^{3+} and Pc^{2-}/Pc^{3-} transformations are reversible processes taking place without substantial structural changes. For describing the postwave in the case of oxidation of central metal ion, formation and oxidation of dimeric species were assumed. Pc^{3-}/Pc^{4-} is also a reversible redox process; however, it is accompanied with a phase transition. Pc^{2-}/Pc^{-} transformation can also be realized; however, due to the structural changes, it eventually leads to the delamination/dissolution of the FePc layer. The mass changes during the redox transformations can be elucidated by considering the sorption-desorption of counterions and water molecules in/from the FePc layer. The pH dependence of the peak potentials of all processes that are related to the redox reactions of the Pc ring revealed that protonation and deprotonation reactions also occur. It has also been proven that adducts with O_2 are formed. The reduction of oxygen starts when Fe^{3+} ions of FePc had been converted to Fe^{2+} during reduction.

Acknowledgments Financial support of the National Scientific Research Fund (OTKA K100149) is gratefully acknowledged. One of the authors (Á. Nemes) is grateful for the support of the European Union and the State of Hungary, co-financed by the European Social Fund in the framework of TÁMOP 4.2.4. A/-11-1-2012-0001 National Excellence Program.

References

1. Linstead RP (1934) Phthalocyanines. Part I. A new type of synthetic colouring matters. J Chem Soc 1016–1017
2. Dent CE, Linstead RP, Lowe AR (1934) Phthalocyanines. Part VI. The structure of the phthalocyanines. J Chem Soc 1033–1039
3. Lever ABP, Wilshire JP (1976) Redox potentials of metal phthalocyanines in non-aqueous media. Can J Chem 54:2514–2516
4. Leznoff CC, Lever APB (eds) (1989–1996) Phthalocyanines: properties and applications. VCH Publ., New York, vols 1–4
5. Nikolić BZ, Adzić RR, Yeager EB (1979) Reflectance spectra of monolayers of tetrasulfonated transition-metal phthalocyanines adsorbed on electrode surfaces. J Electroanal Chem 103:281–287
6. Zagal J, Bindra P, Yeager E (1980) A mechanistic study of O_2 reduction on water soluble phthalocyanines adsorbed on graphite electrodes. J Electrochem Soc 127:1506–1517
7. Simic-Glavaski B, Zecevic S, Yeager E (1983) Study of phthalocyanines in aqueous-solutions and adsorbed on electrode surfaces. J Electroanal Chem 150:469–479
8. Scherson DA, Yao SB, Yeager EB, Eldridge J, Kordesch ME, Hoffman RW (1983) In situ and ex situ Mössbauer-spectroscopy studies of iron phthalocyanine adsorbed on high surface-area carbon. J Phys Chem 87:932–943
9. Collins GCS, Schiffrin DJ (1985) The properties of electrochromic film electrodes of lanthanide diphthalocyanines in ethylene glycol. J Electrochem Soc 132:1835–1842
10. Kahl JL, Faulkner LR, Dwarakanath K, Tachikawa H (1986) Reversible oxidation and reduction of magnesium phthalocyanine electrodes. Electrochemical behavior and in situ Raman spectroscopy. J Am Chem Soc 108:5434–5440
11. Elzing A, Van der Putten A, Visscher W, Barendrecht E (1987) The cathodic reduction of oxygen at metal tetrasulfonato-phthalocyanines: influence of adsorption conditions on electrocatalysis. J Electroanal Chem 233:99–112
12. Van der Putten A, Elzing A, Visscher W, Barendrecht E (1986) Oxygen reduction on vacuum-deposited and absorbed transition-metal phthalocyanine films. J Electroanal Chem 214:523–533
13. Castaneda F, Plichon V (1987) Electrochemistry of a lutetium diphthalocyanine film in contact with an acidic aqueous medium. J Electroanal Chem 233:77–85
14. Castaneda F, Plichon V (1987) Electrochemical process in electrochromic films of lutetium diphthalocyanine. J Electroanal Chem 236:163–175
15. Paliteiro C, Hamnett A, Goodenough JB (1988) Study of the electroreduction of dioxygen on thin films of platinum phthalocyanine in alkaline solutions: part I. Electrochemical investigations. J Electroanal Chem 239:273–289
16. He P, Lu J, Cha C, Crouigneau, Léger JM, Lamy C (1990) Electrochemical and "in situ" electron spin resonance studies of iron phthalocyanine deposited on carbon electrodes. J Electroanal Chem 290:203–214
17. He P, Crouigneau P, Beden B, Lamy C (1990) "In situ" ESR and UV-visible spectroscopic studies of iron phthalocyanine films deposited on gold electrodes. J Electroanal Chem 290:215–227
18. El Hourch A, Belcadi S, Moisy P, Crouigneau P, Léger JM, Lamy C (1992) Electrocatalytic reduction of oxygen at iron phthalocyanine modified polymer electrodes. J Electroanal Chem 339:1–12
19. Jansen R, Beck F (1994) Electrochemical characterization and transformation of redox states at the surface of metallophthalocyanines. Electrochim Acta 39:921–931
20. Komorsky-Lovrić S (1995) Voltammetry of microcrystals of cobalt and manganese phthalocyanines. J Electroanal Chem 397(1–2):211–215
21. Komorsky-Lovrić S, Lovrić M, Scholz F (1997) Sulfide ion electrooxidation catalysed by cobalt phthalocyanine microcrystals. Microchim Acta 127:95–99
22. Kogan IL, Yakushi K (1998) Electrochemical and spectroelectrochemical properties of a new stable composite film electrode platinum phthalocyanine–poly-bisphenol-A-carbonate. Electrochim Acta 43:2053–2060
23. Jiang J, Kucernak A (2000) Electrochemical impedance studies of the undoping process of platinum phthalocyanine charge transfer microcrystals. J Electroanal Chem 490:17–30
24. Jiang J, Kucernak A (2000) The electrochemistry of platinum phthalocyanine microcrystals: I. Electrochemical behaviour in acetonitrile electrolytes. Electrochim Acta 45:2227–2239

25. Jiang J, Kucernak AR (2001) The electrochemistry of platinum phthalocyanine microcrystals. IV. Temperature dependence of the electrochemical behaviour in non-aqueous solution. Electrochim Acta 46:3445–3456
26. Brown RJC, Kucernak AR (2001) The electrochemistry of platinum phthalocyanine microcrystals: III. Electrochemical behaviour in aqueous electrolytes. Electrochim Acta 46:2573–2582
27. Brown RJC, Kucernak AR, Long NJ, Mongay-Batalla C (2004) Spectroscopic and electrochemical studies on platinum and palladium phthalocyanines. New J Chem 28:676–680
28. Brown RJC, Kucernak AR (2005) The photoelectrochemistry of platinum phthalocyanine films in aqueous media. J Solid State Electrochem 9:459–468
29. Brown RJC, Brett DJL, Kucernak ARJ (2009) An electrochemical quartz crystal microbalance study of platinum phthalocyanine thin films. J Electroanal Chem 633:339–346
30. Geraldo D, Linares C, Chen YY, Ureta-Zanartu S, Zagal JH (2002) Volcano correlations between formal potential and Hammett parameters of substituted cobalt phthalocyanines and their activity for hydrazine electro-oxidation. Electrochem Comm 4:182–187
31. Linares C, Geraldo D, Paez M, Zagal JH (2003) Non-linear correlations between formal potential and Hammett parameters of substituted iron phthalocyanines and catalytic activity for the electro-oxidation of hydrazine. J Solid State Electrochem 7:626–631
32. Caro CA, Zagal JH, Bedioui F (2003) Electrocatalytic activity of substituted metallophthalocyanines adsorbed on vitreous carbon electrode for nitric oxide oxidation. J Electrochem Soc 150:E95–E103
33. Ponce I, Silva JF, Onate R, Rezende MC, Páez MA, Pavez J, Zagal JH (2011) Enhanced catalytic activity of Fe phthalocyanines linked to Au(111) via conjugated self-assembled monolayers of aromatic thiols for O_2 reduction. Electrochem Comm 13:1182–1185
34. Zagal JH, Ponce I, Baez D, Venegas R, Pavez J, Paez M, Gulppi M (2012) A possible interpretation for the high catalytic activity of heat-treated non-precious metal Nx/C catalysts for O_2 reduction in terms of their formal potentials. Electrochem Solid-State Lett 15:B90–B92
35. Mi J, Guo L, Liu Y, Liu W, You G, Qian S (2003) Excited-state dynamics of magnesium phthalocyanine thin film. Phys Lett A 310: 486–492
36. Gaffo L, Goncalves D, Faria RC, Moreira WC, Oliveira ON Jr (2005) Spectroscopic, electrochemical, and microgravimetric studies on palladium phthalocyanine film. J Porphyrins Phthalocyanines 9(1):16–21
37. Gaffo L, Brasil MJSP, Cerdeira F, Giles C, Moreira WC (2005) The effect of cyclic voltammetry on the crystalline order of PdPc thin films. J Porphyrins Phthalocyanines 9:89–93
38. Koca PA, Dincer HA, Kocak MB, Gül A (2006) Electrochemical characterization of Co(II) and Pd(II) phthalocyanines carrying diethoxymalonyl and carboxymethyl substituents. Russ J Electrochem 42:31–37
39. Arici M, Arican D, Lütfi Ugur A, Erdogmus A, Koca A (2013) Electrochemical and spectroelectrochemical characterization of newly synthesized manganese, cobalt, iron and copper phthalocyanines. Electrochim Acta 87:554–566
40. Sakamoto K, Ohno-Okumura E (2009) Syntheses and functional properties of phthalocyanines. Materials 2:1127–1179
41. Yamazaki S, Fujiwara N, Yasuda K (2010) A catalyst that uses a rhodium phthalocyanin for oxalic acid oxidation and its application to an oxalic acid sensor. Electrochim Acta 55:753–758
42. Kim S, Ohta T, Kwag G (2000) In situ structural investigation of iron phthalocyanine monolayer adsorbed on electrode surface by X-ray absorption fine structure. Bull Korean Chem Soc 21:588–594
43. Yuan Y, Zhao B, Jeon Y, Zhong S, Zhou S, Kim S (2011) Iron phthalocyanine supported on amino-functionalized multi-walled carbon nanotube as an alternative cathodic oxygen catalyst in microbial fuel cells. Bioresour Technol 102:5849–5854
44. Akinbulu IA, Ozoemena KI, Nyokong T (2011) Formation, surface characterization, and electrocatalytic application of self-assembled monolayer films of tetra-substituted manganese, iron, and cobalt benzylthio phthalocyanine complexes. J Solid State Electrochem 15(10):2239–2251
45. Selvaraj C, Munichandraiah N, Scanlon LG (2012) Dilithium phthalocyanine as a catalyst for oxygen reduction in non-aqueous Li-O_2 cells. J Porphyrins Phthalocyanines 16:255–259
46. Ogunsipe AO, Idowu MA, Ogunbayo TB, Akinbulu IA (2012) Protonation of some non-transition metal phthalocyanines—spectral and photophysicochemical consequences. J Porphyrins Phthalocyanines 16:885–894
47. Guo J, He H, Chu D, Chen R (2012) OH−-binding effects on metallophthalocyanine catalysts for O_2 reduction reaction in anion exchange membrane fuel cells. Electrocatalysis 3:252–264
48. Alpatova NM, Ovsyannikova EV (2011) Electropolymerization of phthalocyanines. In: Cosnier S, Karyakin A (eds) Electropolymerization. Wiley, Weinheim, pp 111–132
49. Yuan Y, Ahmed J, Kim SH (2011) Polyaniline/carbon black composite-supported iron phthalocyanine as an oxygen reduction catalyst for microbial fuel cells. J Power Sources 196:1103–1106
50. Xing R, Wu L, Fei ZH, Wu P (2013) Palladium phthalocyaninesulfonate functionalized mesoporous polymer: a highly efficient photocatalyst for degradation of 4-chlorophenol under visible light irradiation. J Mol Catal A Chem 371:15–20
51. Lu A, Fang YY, Zhu M, Huang S, Ou ZP, Kadish KM (2012) Dioxygen reduction catalyzed by substituted iron tetraphenylporphyrins in acidic media. J Porphyrins Phthalocyanines 16:310–315
52. Baranton S, Coutanceau C, Garnier E, Léger J-M (2006) How does α-FePc catalysts dispersed onto high specific surface carbon support work towards oxygen reduction reaction (orr)? J Electroanal Chem 590:100–110
53. Nemes Á, Moore CE, Inzelt G (2013) Electrochemical and nanogravimetric studies of palladium phthalocyanine microcrystals. J Serb Chem Soc 78:2017–2037
54. Baker R, Wilkinson DP, Zhang J (2008) Electrocatalytic activity and stability of substituted iron phthatalocyanines towards oxygen reduction evaluated at different temperatures. Electrochim Acta 53:6906–6919
55. Scholz F, Schröder U, Gulaboski R (2005) Electrochemistry of immobilized particles and droplets. Springer, Berlin, p 114
56. Inzelt G (2010) Electrochemical quartz crystal nanobalance. In: Scholz F (ed) Electroanalytical methods, 2nd edn. Ch. II. 10, Springer, Berlin, pp 257–270
57. Snook GA, Bond AM, Fletcher S (2002) The use of massograms and voltammograms for distinguishing five basic combinations of charge transfer and mass transfer at electrode surface. J Electroanal Chem 526:1–9
58. Suárez MF, Bond AM, Compton RG (1999) Significance of redistribution reactions detected by in situ atomic force microscopy during early stages of fast scan rate redox cycling experiments at a solid 7,7,8,8-tetracyanoquinodimethane-glassy carbon electrode-aqueous (electrolyte) interface. J Solid State Electrochem 4:24–33
59. Evans CD, Chambers JQ (1994) Electrochemical quartz crystal microbalance study of tetracyanoquinodimethane conducting salt electrodes. Chem Mater 6:454–460
60. Inzelt G, Németh K, Róka A (2007) Electrochemical quartz crystal microbalance study of redox transformations of TCNQ microcrystals in concentrated LiCl solutions. Electrochim Acta 52:4015–4023
61. Inzelt G, Róka A (2008) Electrochemical nanogravimetric studies of ruthenium(III) trichloride microcrystals. Isr J Chem 48:185–197
62. Bond AM, Fletcher S, Symons PG (1998) The relationship between the electrochemistry and the crystallography of microcrystals. The case of TCNQ (7,7,8,8,-tetracyanoquininodimethane). Analyst 123: 1891–1904